Measurement of food dehydration during freezing in mechanical and cryogenic freezing conditions

Violette Mulot, Hayat Benkhelifa, Didier Pathier, Fatou-Toutie Ndoye, Denis Flick

Measurement of food dehydration during freezing in mechanical and cryogenic freezing conditions

Violette MULOT[a,b,c], Hayat BENKHELIFA[a,b], Didier PATHIER[c], Fatou-Toutie NDOYE[a], Denis FLICK[a,b]

[a]IRSTEA, Génie des Procédés Frigorifiques (GPAN)
Antony, F-92160, France, violette.mulot@irstea.fr, +33 1 40 96 65 48
[b]AgroParisTech, Inra, Université Paris-Saclay,
UMR Ingénierie, Procédés, Aliments (GENIAL)
Massy, F-91300, France
[c]Air Liquide, Paris Innovation Campus
Jouy-en-Josas, F-78350, France

ABSTRACT

The freezing of unpackaged foods induces water loss due to interactions with the surrounding medium. The weight loss resulting from this dehydration is up to 6 % according to the product and the freezing process. Food dehydration was studied for various operating conditions from mechanical to cryogenic ones with the same freezing device using Tylose as a food model material. The dehydration was studied for several surface states (smooth or streaked surface) and product porosities (full or perforated plates). It was found that weight loss is estimated with a good reproducibility in the developed freezer. The influence of freezing operating conditions and product characteristics on weight loss were clearly pointed out. From these results, weight loss could be related to the surface temperature evolution. In any case, these results confirm that to limit the weight loss, it is essential to decrease as quickly as possible the surface temperature of the product.

Keywords: Food dehydration; Weight loss; Freezing cabinet; Freezing; Cryogenic.

1. INTRODUCTION

Freezing is widely used for preservation in the food industry because it guarantees long preservation with relatively low impact on product quality. Two types of transfers occur during the freezing of unwrapped products:

- Heat transfer: the product in contact with cold air releases energy to the surrounding environment. This leads to a temperature gradient in the product inducing a heat transfer from its core to its surface and phase change (water crystallization) until reaching thermal equilibrium.
- Water transfer: the water vapor concentration in the surrounding air is lower than the water vapor concentration in the air in equilibrium with the product surface. Thus, a water transfer occurs between the product and its surroundings. As for heat transfer, a water concentration gradient

appears in the product inducing a water transfer from its core to its surface and then to its surroundings. During the pre-cooling stage, water evaporates from the surface. When ice is formed, it sublimates from the surface causing the emergence of a dehydrated layer.

Dehydration during freezing implies a loss of quality especially within the dehydrated layer but also weight loss which means financial losses for industrials. Dehydration is strongly influenced by the product type, its initial temperature and the freezing process.

To predict weight loss in food during freezing, numerical solving of heat and mass transfer equations led to several models (Andreasen, 2009; Campanone et al., 2005; Campañone et al., 1998; Pham, 2006; Pham and Willix, 1984; Rouaud and Pham, 2012; Tocci and Mascheroni, 1995). From these numerical models, simplified ones were also proposed (Campañone et al., 2001). All these models are valuable decision tools for selecting one technology (characterized by its range of temperature and air velocity) relatively to another in order to freeze a given product and limit its weight loss.

Models were validated and enriched with experimental data of freezing time and weight loss during freezing which help better understand transfer phenomena. Meat and fish products were widely studied (Boonsumrej et al., 2007; Bustabad, 1999; Campanone et al., 2002; Espinoza Rodezno et al., 2013; Lambrinos and Aguirre-Puente, 2003; Pham and Willix, 1984). Few studies focus on highly porous products like pre-baked bread (Hamdami et al., 2004a, 2004b).

For these experimental studies, usually, a given product was placed in a freezer where the temperature and air velocity were controlled and measured. Air relative humidity was sometimes also measured but not controlled. Temperature in the product was measured during freezing and the product was weighed before and after freezing or sometimes during freezing (Campanone et al., 2002). Most of the time, studies also took into account weight loss during the storage of the frozen products.

These studies highlight the fact that the product weight loss is closely linked to the freezing rate. Most of them compare freezing rates in the mechanical freezing field: air temperature between -15°C and -50°C and air velocity between 0 and 5 m s^{-1}. The air temperature has a high impact on weight loss whereas air velocity does not greatly influence it. A lower air temperature decreases the weight loss.

Few studies differentiate the two main categories of freezing processes: mechanical freezing and cryogenic freezing (Boonsumrej et al., 2007; Espinoza Rodezno et al., 2013; Rouaud and Pham, 2012). Mechanical freezing relates to slower freezing rates than cryogenic one. Indeed, cryogenic freezing allows reaching very low temperature (-78.5°C with CO_2 and -195.8°C with nitrogen) and fast freezing rates. Boonsumrej et al. (2007) used CO_2 cryogenic freezing with a cabinet temperature of -59°C. Only Espinoza Rodezno et al. (2013) used nitrogen injection that allowed reaching cryogenic temperatures from -70°C to -100°C. Nevertheless, both studies used two different types of technologies to study respectively mechanical and cryogenic freezing.

Moreover, the sample was taken out of the freezer to perform the weighing at the end of freezing, thus causing high mass variation.

The aim of the present work is to study the food dehydration during freezing in mechanical and cryogenic freezing conditions. For this, a reliable laboratory scale freezing cabinet was developed to study the total weight loss but also the variation of weight loss with time during the freezing process. It is able to simulate both mechanical and cryogenic freezing conditions in terms of temperature (using liquid nitrogen) and flow velocity. The product is weighed directly in the cold medium during freezing without taking it out of the freezing cabinet. This study presents experiments with Tylose (constant formula of water and methylcellulose) and the dehydration is studied for several food characteristics: the effect of the surface state by using smooth or streaked surface, the effect of the product porosity by using full plates or perforated plates and the effect of the initial temperature. Core temperature, surface temperature and total weight loss results are presented for different freezing conditions in mechanical and cryogenic freezing fields.

2. MATERIALS AND METHODS

2.1. Freezing equipment

A freezing cabinet was developed to recreate both mechanical and cryogenic freezing conditions in terms of temperature and gas flow velocity. Figure 1 presents the operating diagram of this designed freezer. Temperature is adjustable from room temperature to -100°C using a nitrogen injection coupled with a temperature measurement with a Pt100. The gas flow velocity is adjustable from 0 to 9 m s^{-1} thanks to a variable frequency fan connected to a differential pressure measurement with a Pitot tube.

A cold gas flow over a length of 2.8 m is obtained with the designed freezing cabinet. Samples are located in the measuring zone (Figure 1) during experiments. This zone is as far as possible over-the gas flow length to get a well-established and uniform flow (temperatures and velocities). Some meshes were added before and after the measuring zone to homogenize this flow.

As liquid nitrogen is injected for the temperature control, there is no humidity in the freezing cabinet and relative humidity is close to 0.

2.2. Freezing cabinet characterization

Gas flow velocity, temperature, and heat transfer coefficient were measured in the measuring zone of the freezing cabinet in order to check their uniformity near sample locations. For these measurements, no samples were placed in the measuring zone.

Gas flow velocity

First, gas flow velocity was measured in the median plane of the measuring zone (Figure 1). A mapping was made to cover the entire width and height of this flow section with 30 measuring points, this mapping is presented on Figure 2.

Flow velocity measurements were carried out at 20°C with a hot-wire anemometer (0-50 m s^{-1}, Velocicalc®, 9565). For each measuring point, 3 velocity readings were made. The fan motor was adjusted at its maximum rotational speed during all these measurements in order to verify the velocity uniformity and stability over time in the worst case.

Temperature

Then, temperature measurements were made in the median plane of the measuring zone at mid-height position, 3 equidistant calibrated type-T thermocouples (precision 0.1°C) were placed across the width of the flow section, on the left, on the middle and on the right position. For these measurements, flow velocity was fixed at 3.5 m s^{-1} and four temperatures were checked: 0°C, -30°C, -50°C and -100°C (whole temperature range of the freezing cabinet). Temperature was recorded for 360 s after stabilization of the freezing cabinet.

Heat transfer coefficient

Finally, convective heat transfer coefficients (*HTC*) were measured at mid-height position in the median plane of the measuring zone. For these measurements, three equidistant devices were placed along the width of the flow section (left, middle and right position). The devices are composed of a copper plate (50×50 mm) which is heated by an electrical resistance and insulated underneath. For each one, two type-T thermocouples measure the temperature of the copper surface and the gas temperature above it. A programmable controller performs temperature recording and flux calculation (Eckert and Goldstein, 1976).

Three flow velocities were studied: 4.2, 6.6 and 8.4 m s^{-1}, temperature was set at 15°C. Heat transfer coefficients were recorded for 120 s once the freezing cabinet was stabilized.

2.3. Samples, sample temperature and sample weight

Sample preparation

To study food dehydration during freezing, Tylose plates (23 % methylcellulose, 76.4 % water and 0.5 % sodium chloride) were used as a model material (length=80 mm, width=45 mm, thickness=18 mm, mass=70.7-73.8 g). Their lateral faces were insulated with 1-cm-thickness (e) expanded polystyrene (λ_p=*0.033* W m^{-1} K^{-1}) in order to consider quite only 1D heat and mass transfers. The lateral conductance, can be estimated from the lateral area of the product ($S_{lateral}$), the convective heat transfer coefficient (*HTC*) and the insulation thermal resistance: $\frac{S_{lateral}}{\frac{1}{HTC}+\frac{e}{\lambda_p}}$. The conductance through the upper and lower surface ($S_{upper/lower}$) is: $S_{upper/lower}\,HTC$.

Since for the measured *HTC* values, the lateral conductance is less than 4 % of the upper/lower conductance, the lateral heat flux should be very low compared to the upper/lower ones. Using the chart proposed by Cleland et

al. (1994), it was also found that the difference of freezing time with the ideal 1D case should be less than 4 %.

Three types of Tylose plate and surface state were studied (Figure 3): full plates with smooth surfaces (Figure 3a, initial temperature T_i=*20*°C and T_i=*5*°C), full plates with streaked surfaces (Figure 3b, initial temperature T_i=20°C) and perforated plates with smooth surfaces (Figure 3c, initial temperature T_i=*20*°C). To obtain streaked surfaces, the upper and lower surfaces of the Tylose block were scrapped with a saw blade. This type of surface aims to simulate products with rough surfaces, for example frozen patties. Perforated plates were made doing a regular perforation using a punch. This type of macro-porosity is found in product whose permeability is preferentially oriented in one direction (vertical) like blinis. It does not model micro-porous food as sponge cakes. The air/product interface area is increased by about 16 % for the streaked surface and about 41 % for the perforated plate . This different Tylose plates can be used as food model materials, with different surface states and different porosities.

In the freezing cabinet, samples were located in the median plane of the measuring zone (Figure 1) at mid-height position (Figure 4). Three samples were placed per run in the freezing cabinet on the left, on the middle and on the right position, they were separated equidistantly across the width of the measuring zone.

Sample temperature and sample weight

For temperature recording in the sample, two calibrated type-T thermocouples (precision 0.1°C) were used per sample, one dedicated for the upper surface temperature recording (1 mm under the upper surface) and the other for the core temperature recording. They were equipped with a needle so that they could be accurately positioned and inserted from the sample lateral side along likely isotherms, so that conduction along the thermocouples is minimized.

For weighing, two scales were used: Mettler Toledo® PG1003S and Sartorius® QUINTIX3102-1S. The weighing precision is 0.01 g. Scales were fitted with hangers for below-the-balance weighing. Thus, scales are kept outside the freezing cabinet while samples are in the cold zone.

2.4. Weight loss and water vaporization during food freezing

Weight loss is due to water vaporization from the product surface to the surroundings. The weight loss variation with time during freezing can be determined from the integral of the water vapor flux from the product surface over time (Phimolsiripol et al., 2014). The water vaporization flux (evaporation or sublimation) at the product surface (φ_{vap}) is expressed with Equation (1).

$$\varphi_{vap} = h_m S(C_{vap-eq} - C_{vap-sur}) \quad (1)$$

where h_m is the external mass transfer coefficient and S the exchange area. $C_{vap\text{-}eq}$ is the water vapor concentration in equilibrium with the product surface. $C_{vap\text{-}sur}$ is the water vapor concentration in the surrounding gas.

C_{vap-eq} is estimated from the water activity at the product surface (a_{ws}) and the saturation water vapor concentration C_{vsat} at the product surface temperature T_s thanks to Equation (2).

$$C_{vap-eq} = a_{ws}\, C_{vsat(T_s)} \quad (2)$$

$C_{vap-sur}$ is estimated from the relative humidity (*RH*) in the cold environment and the saturation water vapor concentration at the gas temperature T_g thanks to Equation (3).

$$C_{vap-sur} = RH\, C_{vsat(T_g)} \quad (3)$$

2.5. .Experimental procedure

First of all, experiments were made to measure the time required for thermal center of Tylose full plates with smooth surfaces (T_i=*20*°C) to reach -18°C. This step was necessary to ensure that the left, middle and right samples were submitted to the same freezing conditions. Three replicates were made for the seven operating conditions. For a freezing run, when gas set point temperature and gas flow velocity were stable in the freezing cabinet, three samples, fitted with type-T thermocouples at core, were introduced in the freezing cabinet. Core temperatures of the three samples were recorded until they reached -18°C.

Secondly, Tylose plate dehydration due to freezing process was studied by measuring the total weight loss for the four types of plates. For a freezing run, two samples were dedicated to the weight recording (left and right samples) whereas the third one (middle sample) was used for core and upper surface temperature recording. When operating conditions reached the stationary regime, process ventilation and nitrogen injection were switched off and samples were introduced in the freezing cabinet (Figure 4). The initial masses of samples suspended inside the cabinet were measured ($M_{0suspended}$). Then, process ventilation and nitrogen injection were switched on. The freezing time is the time for the thermal center of the middle sample to reach -18°C. At the end of freezing, the freezing cabinet was switched off and the final masses of samples suspended inside the freezing cabinet were measured ($M_{fsuspended}$). The total relative weight loss (*WL* in %) was calculated using Equation (4).

$$WL = 100\,\frac{M_{0suspended} - M_{fsuspended}}{M_{0Tylose}} \quad (4)$$

$M_{0Tylose}$ is initial Tylose sample mass before freezing.

For full plates with smooth surfaces and an initial temperature of 20°C, seven freezing operating conditions (3 replicates, 6 weight loss measurements) were studied, three temperatures: -30°C, -50°C and -100°C and three gas flow velocities: 3 m s^{-1}, 3.9 m s^{-1} and 7.7 m s^{-1}. For full plates with smooth surfaces and T_i=*5*°C, full plates with streaked surfaces (T_i=*20*°C) and perforated plates with smooth surfaces (T_i=*20*°C), two extreme freezing operating conditions (1 replicate, 2 weight loss measurements) were studied: -30°C, 3.9 m s^{-1} and -100°C, 3.9 m s^{-1} (Table 1).

Finally, the weight loss variation during the freezing of full plates with smooth surfaces (T_i=*20*°c) was studied by measuring weight loss at regular time steps for the freezing operating condition -30°C, 3.9 m s^{-1} (3 replicates).

The protocol is the same as for the measurement of the total weight loss, but two intermediate weighing were performed: after 15 minutes and 30 minutes of freezing. The relative weight loss at each time step was still calculated using Equation (4). An additional experiment was done with 4 intermediate weighing (after 5, 10, 15 and 30 minutes) to validate the weight loss variation trend over time. Nevertheless, too many ventilation and nitrogen injection stops during weighing may disturb the freezing process.

3. RESULTS AND DISCUSSION

3.1. Freezing cabinet characterization

Gas flow velocity

The gas flow velocity results are summarized in Table 2. They show a very good repeatability between the three measurements of each measuring points (standard deviation<0.1) which means a good stability of the velocity for a same position over replicates and over time. Besides, for the upper and bottom wall, horizontal profiles show slightly lower velocities with higher variations (shaded part of Table 2). However, uniform horizontal and vertical profiles are noticeable at mid-height positions (unshaded part of Table 2) where samples are located during freezing which means that the three samples placed at three different horizontal positions are frozen with the same gas flow velocity.

Temperature

The temperature uniformity and stability over time at mid-height position in the measuring zone are summarized in Table 3. The standard deviation of each temperature recording is very low which indicates a good stability and a good temperature regulation system with measured temperatures close to set points. Moreover, results show temperature uniformity between the three positions (left, middle and right position) for a same temperature set point.

Heat transfer coefficient

Measurements with fluxmeters permit characterizing the stability over time and the uniformity of the convective heat transfer coefficient (*HTC*) between the three sample locations. Results are presented in Table 4. For each velocity set point, the standard deviation of each *HTC* recording is low relative to the average value which indicates a good stability over time. Moreover, *HTC* variations are not significant between the three positions. These results validates the *HTC* uniformity and stability at a selected velocity set point where samples are located in the freezing cabinet.

Core temperature - Freezing time

The time required for the thermal center to reach -18°C in the case of full plates with smooth surfaces (T_i=*20*°C) was measured for seven operating conditions (3 replicates) and is defined as the freezing time. Table 5 presents,

for each operating condition, the average freezing time with the standard deviation between the three replicates of each position and the average freezing time with the standard deviation between the three positions (9 replicates).

Whatever the operating conditions, the standard deviation between the three replicates of a same position is low relative to the total freezing time meaning a good repeatability between the three replicates. These results validate the fact that the designed freezing cabinet can be reliably used to repeat freezing tests under same operating conditions. Moreover, for same operating conditions, standard deviation is also low relative to the average freezing time between the three positions. This means that the three samples placed per freezing run are frozen in the same way.

These results coupled with those of the operating conditions uniformity and stability (gas flow velocity, temperature and heat transfer coefficient, Table 2, Table 3 and Table 4) validate identical and stable freezing conditions with a similar thermal treatment whatever the sample lateral position at mid-height of the measuring zone.

3.2. Total weight loss

Once the freezing equipment was validated, experiments were done with four types of Tylose plate to study total weight loss due to freezing process. Table 6 presents, for each operating condition the total relative weight loss (*WL*) when core temperature reaches -18°C.

Whatever the type of Tylose plate and operating conditions, results show a good repeatability between replicates with low standard deviations.

Figure 5a presents results of total relative weight loss for Tylose full plates with smooth surfaces (T_i=*20*°c) as a function of the gas temperature and the gas flow velocity. Figure 5b presents the total relative weight loss for the four types of plate as a function of the gas temperature (gas flow velocity=3.9 m s^{-1}).

Influence of the freezing operating conditions

On both graphs of Figure 5, whatever the gas flow velocity and the type of plate, a large influence of the gas temperature on the weight loss is noticeable, the lower the gas temperature, the lower the weight loss. Decreasing the gas temperature from -30°C to -100°C divides the total relative weight loss by 1.9 to 3.4 as a function of the type of plate.

Nevertheless, the influence of the gas flow velocity is less pronounced. Actually, increasing the flow velocity has opposite effects which compensate each other. On the one hand, increasing the flow velocity leads to shorter freezing time with a larger *HTC*; on the other hand, the mass transfer coefficient is also larger which leads to faster water loss rates. The influence of the gas flow velocity seems to be more significant at lower gas temperature. For high freezing temperatures, the gas flow velocity has no influence on the weight loss, whereas, for lower freezing temperatures, a higher flow velocity reduces the total relative weight loss (Figure 5a).

Influence of the initial temperature

The initial temperature of the product has a great influence on weight loss. For full plates with smooth surfaces, decreasing the initial temperature from 20°C to 5°C allows decreasing the total weight loss of 22 % for the operating conditions -30°C, 3.9 m s^{-1} and 46 % for the freezing condition -100°C, 3.9 m s^{-1}. Indeed, with a lower initial temperature, the total freezing time is shorter which decreases the total relative weight loss. The water evaporation kinetics at the product surface during the pre-cooling stage can mainly explain the weight loss reduction. This stage is shorter for $T_i=5$°C than for $T_i=20$°C because the initial temperature is closer to the initial freezing temperature (around -1.5°C) for Tylose as shown on Figure 6.

Influence of the type of Tylose plate

The freezing of full plates with streaked surfaces and perforated plates with smooth surfaces were studied. Perforated plates aim to simulate a porous matrix. Both types of plate have larger exchange surfaces with the surrounding media than the full plate with smooth surfaces: +16 % for the streaked surface and +41 % for the perforated plate. On the one hand, heat transfer is facilitated so that the freezing time decreases, but, on the other hand, a larger surface leads to more water vaporization. Streaking the surface leads to a relative weight loss 1.1 times higher at -30°C and 1.3 times higher at -100°C for a respective freezing time 1.3 times lower and 1.2 times lower. Perforating the plate leads to a relative weight loss 1.1 times higher at -30°C and 1.2 times higher at -100°C for a freezing time 1.4 times lower for both cases. As the freezing time is enough reduced streaking the surface or perforating the plate, the weight loss does not significantly increase.

3.3. Variation of weight loss with time

The variation of weight loss with time was studied for full plates with smooth surfaces and for the freezing condition -30°C, 3.9 m s^{-1} (3 replicates). Two intermediate weighing were done at 15 minutes and at 30 minutes whereas the total freezing time is 45 min. An additional experiment with four intermediate weighing (after 5, 10, 15 and 30 minutes) was also carried out. Figure 7 shows the results of variation of weight loss during freezing for the two samples dedicated to the weight recording (left and right). The evolution of the surface temperature with time is represented on each graph. Results show repeatable experiments between replicates and between the two samples of a same run. For the experiment with four intermediate measurements, the values at 15, 30 and 45 minutes are slightly lower than for the experiments with only 2 intermediate measurements. Indeed, the two additional operating stops at the beginning of the freezing process slow down the weight loss kinetics but this experiment validates the nonlinear trend of the variation of weight loss with time during the freezing process.

On each graph, trends of weight loss variation with time are similar: the weight loss rate is high at the beginning of freezing and gradually slows down until the end of the freezing process. Based on the three experiments with the two intermediate weighing, during the first 15 minutes of freezing, 61 % of the global freezing weight loss is

reached, then, 27 % from 15 minutes to 30 minutes and 12 % from 30 minutes to the end of the freezing process. This trend is closely related to the surface temperature variation as it is shown in section 3.4.

3.4. Relation between weight loss and surface temperature

Variation of weight loss with time and surface temperature

In this part, measured weight loss variation with time and total weight loss are linked to the surface temperature variation as a function of the freezing time thanks to the theory presented in Section 2.4.

Considering Equation (1), $C_{vap\text{-}sur}$ and $C_{vap\text{-}eq}$ must be determined. In our case, the water vapor concentration in the cold environment, $C_{vap\text{-}sur}$, Equation (3), is constant and close to 0 during the freezing process since nitrogen is continuously injected in the freezing cabinet ($RH=0$). Considering $C_{vap\text{-}eq}$, Tylose (like the majority of food) is mainly composed of water, so, the water activity at the product surface (a_{ws}) is initially close to one. Thus, based on Equation (2), $C_{vap\text{-}eq}$ is equal to $C_{vsat(Ts)}$ that is calculated with Clausius-Clapeyron (Corriou, 1985) and ideal gas equations considering the surface temperature variation during freezing. Figure 8a presents the variations of surface temperature T_s and calculated $C_{vsat(Ts)}$ versus freezing time for a full plate with smooth surfaces (-30°C, 3.9 m s^{-1}). C_{vsat} decreases in the same way as the surface temperature.

From the simplification of Equation (1), the integral of the vaporization flux which is equal to the weight loss at time t can be calculated with Equation (5).

$$WL_{(t)} = h_m S \int_0 C_{vsat(T_s)} dt \quad (5)$$

Thus, weight loss should be proportional to the integral of $C_{vsat(Ts)}$ over time. The integral curve of $C_{vsat(Ts)}$ has a trend comparable to the curve of weight loss variation with time (Figure 8b). Figure 8c shows the linear relation between the relative weight loss and the integral of $C_{vsat(Ts)}$ which is related to the surface temperature ($R^2=0.995$).

In conclusion, the variation of the relative weight loss during freezing is strongly linked to the variation of the product surface temperature and contains 3 steps during the freezing process. At the very beginning of the freezing process, the relative weight loss quickly increases because $C_{vsat(Ts)}$ is high. During the pre-cooling stage, the weight loss rate decreases like $C_{vsat(Ts)}$ (slope of Figure 8b is decreasing between 0 and 6 min). Then, the surface temperature is almost constant during water crystallization as the evaporative flux. Finally, the surface temperature gradually continues decreasing during the sub-cooling stage slower and slower when it approaches the surroundings temperature. During this third stage, the weight loss rate decreases again.

Total weight loss and surface temperature

Figure 9 presents, for different operating conditions, the total weight loss (kg) (when core temperature reaches -18°C) versus the integral of $C_{vsat(Ts)}$ over the total freezing time.

It can be observed, as expected from Equation (5), that the total weight loss is proportional to the integral of $C_{vsat(Ts)}$ over the total freezing time, quite independently of the surrounding temperature and the initial product

temperature. The proportionality coefficient (h_mS) is the slope of the curve. This is why, when the product surface is increased, the slope of the curve increases. It could be also expected that increasing velocity would increase the slope because the mass transfer coefficient h_m should be higher but it is seen that the influence of velocity is not very noticeable as already highlighted in Section 3.2. This could be due to surface dehydration at higher gas velocity that lowers the water activity.

In any case, these results confirm that to limit the weight loss, it is essential to decrease as quickly as possible the surface temperature of the product. Furthermore, knowing the experimental surface temperature variation over freezing time, it is possible to obtain an estimation of weight loss.

4. CONCLUSIONS

In this paper, it was shown that the designed freezing cabinet allows getting uniform and stable operating conditions, in terms of temperature, gas flow velocity and *HTC*.

Various operating conditions were selected to cover the range of mechanical and cryogenic freezing from -30°C, 3.9 m s^{-1} to -100°C, 7.7 m s^{-1} for the study of weight loss of various types of plate. Results show a good repeatability in weight loss measurements between replicates of a same operating condition and between the two sample positions. It was found that the gas temperature has a great influence–weight loss: lowering the temperature decreases weight loss. The gas flow velocity has not a large effect on weight loss at -30°C, but the effect is significant at -50°C and at -100 °C: the weight loss decreases when the flow velocity rises.

The effect of the initial product temperature was also studied: decreasing the initial temperature from 20°C to 5°C allows decreasing the total weight loss by reducing the total freezing time and particularly the pre-cooling stage.

The effect of the product surface state and porosity were studied by considering different exchange surfaces. On the one hand, a larger surface in the case of streaked surfaces and perforated plate leads to more water vaporization but, on the other hand, it also leads to a higher heat transfer and a shorter freezing time. Finally, streaking the surface and perforating the plate do not significantly increase the weight loss.

To finish, the developed freezing cabinet allowed following the variation of weight loss with time for the operating condition -30°C, 3.9 m s^{-1} doing intermediate weighing during freezing. Results coupled with surface temperature reveal a consistent and specific trend. The vaporization rate as the product surface temperature first decreases, during the pre-cooling stage, then, remains almost constant during crystallization and decreases again during the sub-cooling stage.

These data for several food product characteristics and for cryogenic and mechanical freezing conditions will be especially useful to validate numerical models for weight loss prediction during freezing of food considering a water content in the cooling air close to 0. The hygrometry control for mechanical freezing could be an

improvement of the experimental freezing cabinet as in these conditions, water vapor content in the cooling air is not null, leading to lower weight losses.

ACKNOWLEDGEMENTS

The authors gratefully acknowledge the financial support granted by the CIFRE department (Conventions Industrielles de Formation par la Recherche) from the French ANRT (Association Nationale Recherche et Technologie).

NOMENCLATURE

a_{ws}	Water activity
C_{vap-eq}	Water vapor concentration in equilibrium with the product surface (kg m-3)
$C_{vap-sur}$	Water vapor concentration in the cold environment (kg m^{-3})
C_{vsat}	Saturation water vapor concentration (g m^{-3})
e	Thickness of the insulation wall (m)
h_m	External mass transfer coefficient (m s-1)
HTC	Heat transfer coefficient (W m^{-2} K^{-1})
$M_{fsupspended}$	Final suspended sample mass (g)
$M_{0supspended}$	Initial suspended sample mass (g)
$M_{0Tylose}$	Tylose sample mass before freezing (g)
RH	Relative humidity
S	Surface of exchange (m^2)
$S_{lateral}$	Lateral surface of sample plate (m^2)
$S_{upper/lower}$	Upper and lower surface of sample plate (m^2)
t	Time (s)
T_g	Gas temperature in the freezing cabinet (°C)
T_i	Initial temperature (°C)
T_s	Surface temperature (°C)
WL	Relative weight loss (%)
λ_p	Thermal conductivity of polystyrene (W m^{-1} K^{-1})
φ_{vap}	Vaporization flux (kg m^{-2} s^{-1})

REFERENCES

Andreasen, M.B., 2009. Modelling of Heat and Mass Transfer in Food Products, COMSOL Conference, Milan.

Boonsumrej, S., Chaiwanichsiri, S., Tantratian, S., Suzuki, T., Takai, R., 2007. Effects of freezing and thawing

on the quality changes of tiger shrimp (Penaeus monodon) frozen by air-blast and cryogenic freezing. Journal of Food Engineering 80, 292-299.

Bustabad, O.M., 1999. Weight loss during freezing and the storage of frozen meat. Journal of Food Engineering 41, 1-11.

Campanone, L.A., Roche, L.A., Salvadori, V.O., Mascheroni, R.H., 2002. Monitoring of weight losses in meat products during freezing and frozen storage. Food Science and Technology International 8, 229-238.

Campanone, L.A., Salvadori, V.O., Mascheroni, R.H., 2005. Food freezing with simultaneous surface dehydration: approximate prediction of weight loss during freezing and storage. International Journal of Heat and Mass Transfer 48, 1195-1204.

Campañone, L.A., Salvadori, V.O., Mascheroni, R.H., 2001. Weight loss during freezing and storage of unpackaged foods. Journal of Food Engineering 47, 69-79.

Campañone, L.A., Salvadori, Y.O., Mascheroni, R.H., 1998. Finite-difference method to solve coupled heat and mass balances with simultaneous surface dehydration during freezing. Latin American Applied Research 28, 83-88.

Cleland, D.J., Cleland, A.C., Jones, R.S., 1994. Collection of accurate experimental data for testing the performance of simple methods for food freezing time prediction. Journal of Food Process Engineering 17, 93-119.

Corriou, J.P., 1985. Thermodynamique chimique Diagrammes thermodynamiques. Techniques de l'ingénieur Thermodynamique et cinétique chimique base documentaire : TIB323DUO.

Eckert, E.R.G., Goldstein, R.J., 1976. Measurements in heat transfer, 2nd edition ed. Hemisphere Pub. Corp.

Espinoza Rodezno, L.A., Sundararajan, S., Solval, K.M., Chotiko, A., Li, J., Zhang, J., Alfaro, L., Bankston, J.D., Sathivel, S., 2013. Cryogenic and air blast freezing techniques and their effect on the quality of catfish fillets. LWT - Food Science and Technology 54, 377-382.

Hamdami, N., Monteau, J.-Y., Le Bail, A., 2004a. Heat and mass transfer in par-baked bread during freezing. Food Research International 37, 477-488.

Hamdami, N., Monteau, J.-Y., Le Bail, A., 2004b. Simulation of coupled heat and mass transfer during freezing of a porous humid matrix. International Journal of Refrigeration 27, 595-603.

Lambrinos, G., Aguirre-Puente, J., 2003. The weight loss of frozen meat. Experimentation and prediction by using tylose. International Journal of Refrigeration 26, 256-259.

Pham, Q.T., 2006. Modelling heat and mass transfer in frozen foods: a review. International Journal of Refrigeration 29, 876-888.

Pham, Q.T., Willix, J., 1984. Model for food desiccation in frozen storage. Journal of food science 49, 1275-1281.

Phimolsiripol, Y., Love, R.J., Cleland, D.J., 2014. Verification of a simple product weight loss model for refrigerated storage of foods, 3rd IIR International Conference on Sustainability and the Cold Chain, London.

Rouaud, O., Pham, Q.T., 2012. Heat and Mass Transfer Modelling During Freezing of Foodstuffs Comsol Conference, Milan.

Tocci, A.M., Mascheroni, R.H., 1995. Numerical-models for the simulation of the simultaneous heat and mass-

transfer during food freezing and storage. International Communications in Heat and Mass Transfer 22, 251-260.

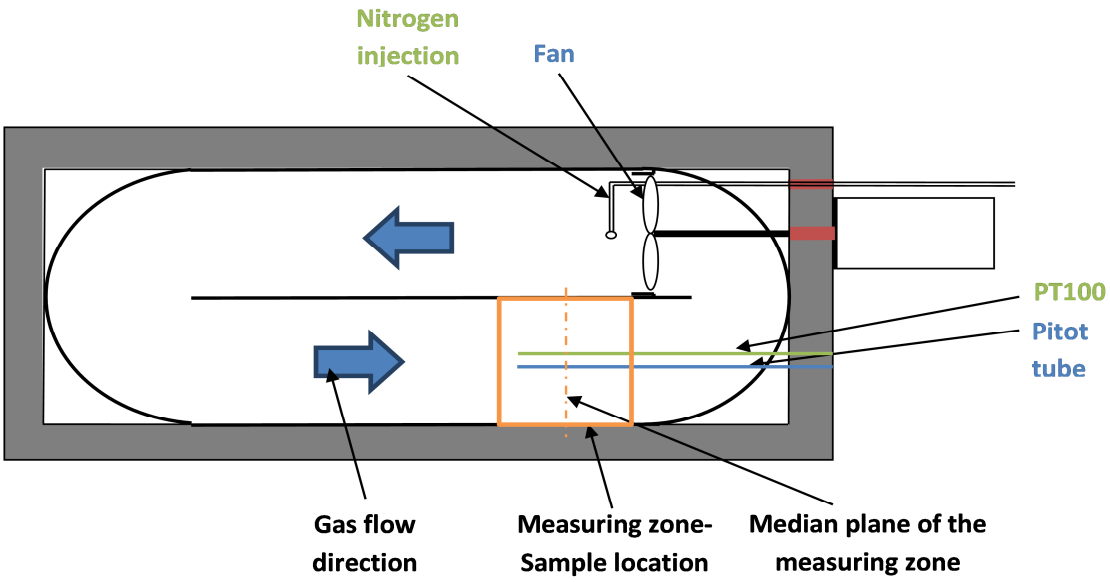

Figure 1: Operating diagram of the freezing cabinet-Top view

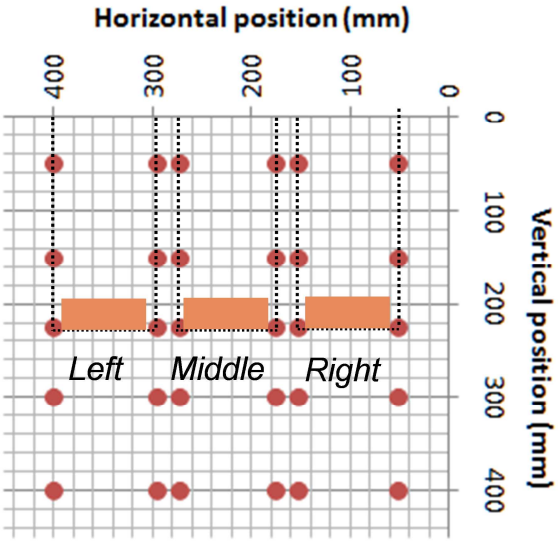

Figure 2: Mapping of the median plane of the measuring zone for flow velocity measurements

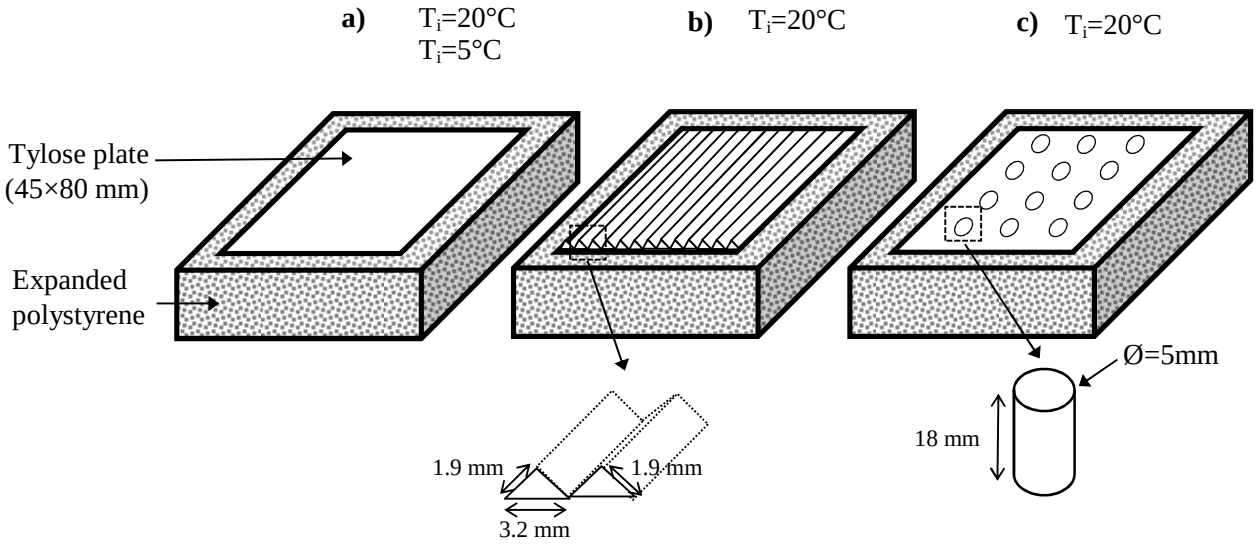

Figure 3: Tylose plates insulated with 1 cm thickness expanded polystyrene
(a) Full plate with smooth surfaces
(b) Full plate with streaked surfaces
(c) Perforated plate with smooth surfaces

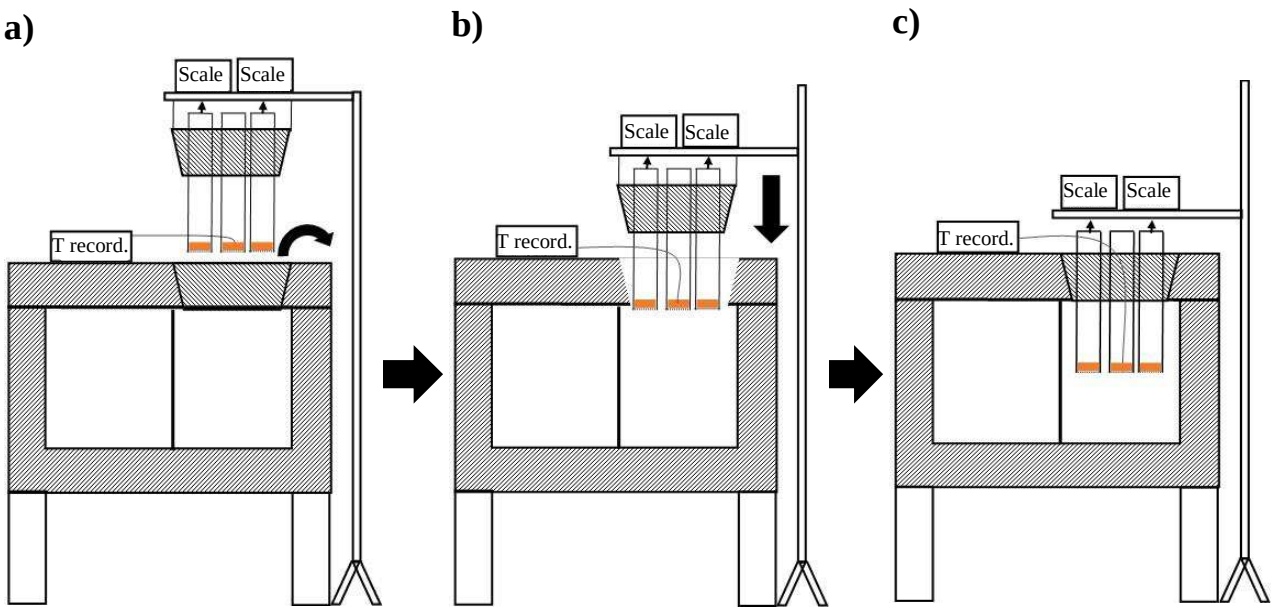

Figure 4: Experimental procedure to introduce samples in the freezing cabinet and measure weight loss during freezing

(a) Opening of the freezing cabinet at stationary regime, ventilation and nitrogen injection are switched off.

(b) Introduction of samples inside the freezing cabinet.

(c)Initial weighing of suspended samples. Then, ventilation and nitrogen injection are switched on.

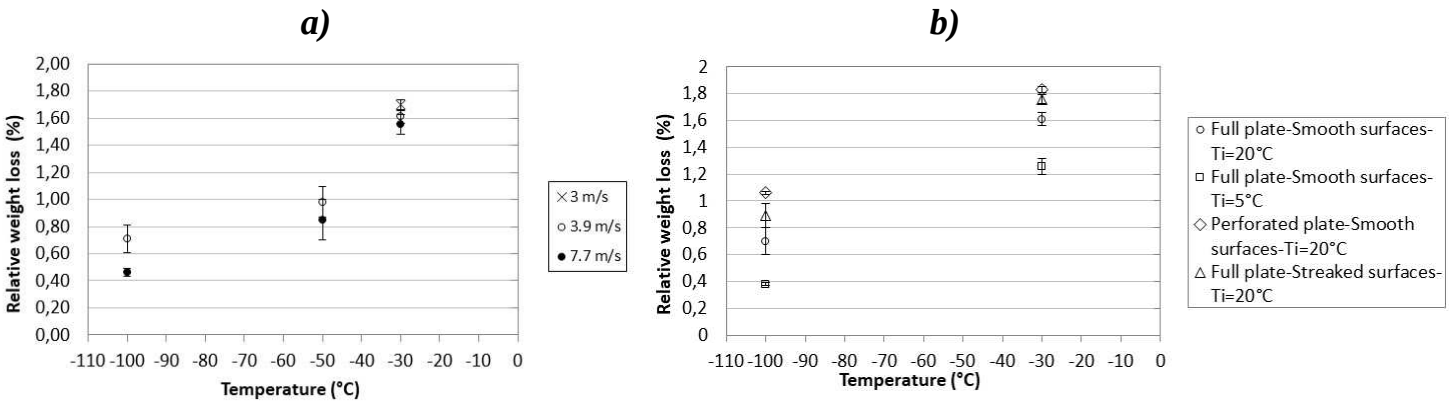

Figure 5: Average total relative weight loss according to gas temperature
***(a)* Tylose full plate with smooth surfaces (T_i=20°C) according to gas flow velocity**
***(b)* Average total relative weight loss according to the type of Tylose plate (gas flow velocity=3.9 m s^{-1})**

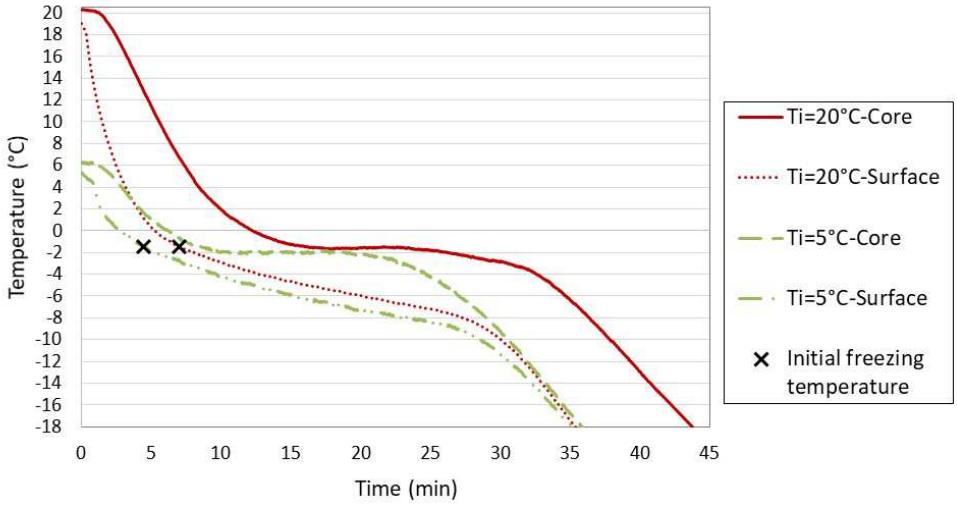

Figure 6: Core and surface temperature kinetics during freezing of full Tylose plate with smooth surfaces and an initial temperature of 20°C or 5°C (operating conditions -30°C, 3.9 m s^{-1})

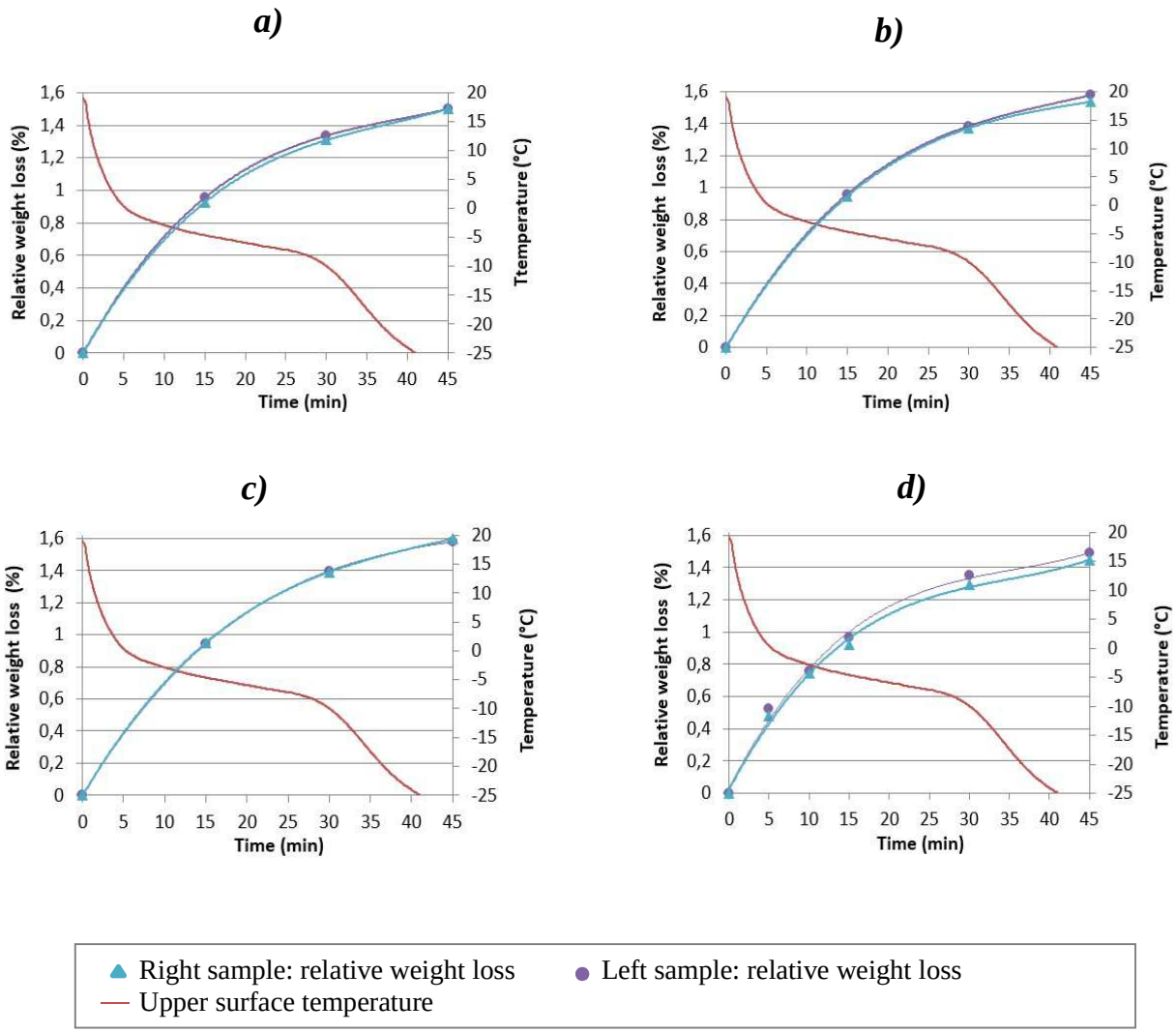

Figure 7: Relative weight loss variation with time and upper surface temperature recording for the freezing operating condition -30°C, 3.9 m s^{-1}
***(a), (b) and (c)* Three replicates with two intermediate weighing**
***(d)* Experiment with four intermediate weighing**

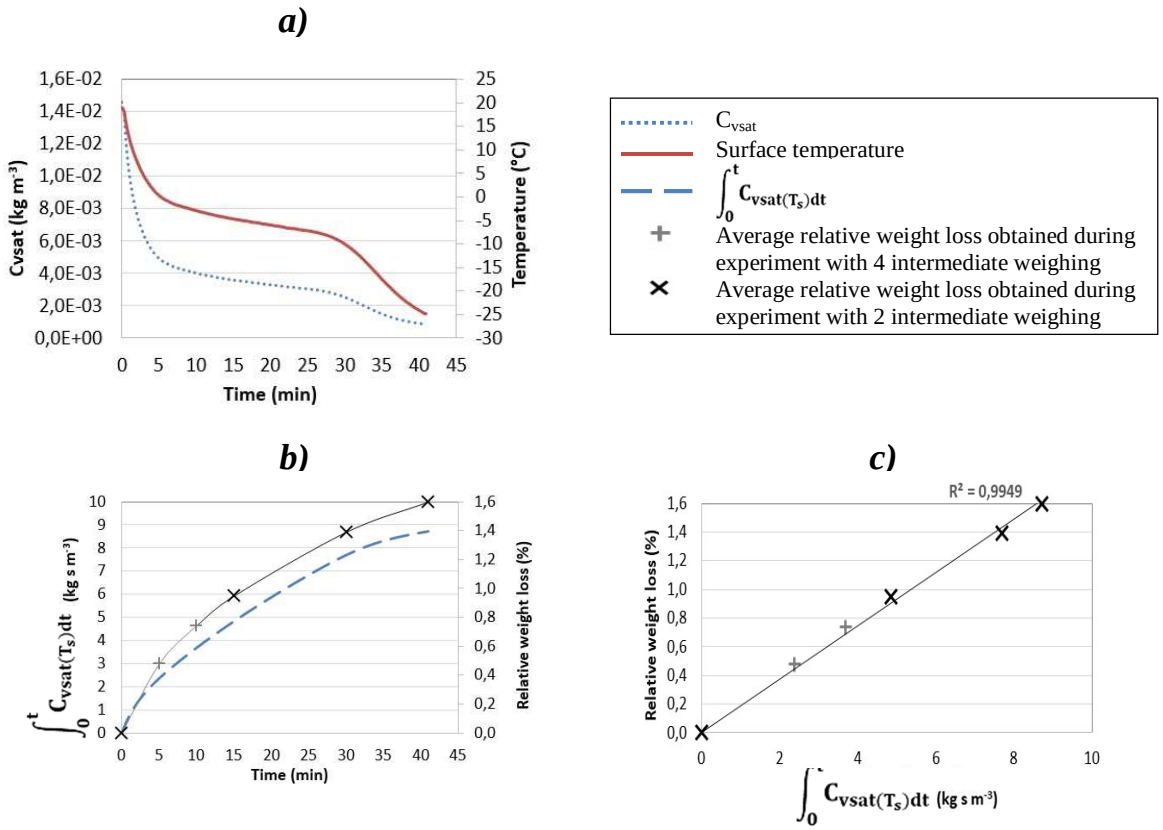

Figure 8: Variation of Tylose surface temperature, calculated saturation water vapor concentration and weight loss during freezing (-30°C, 3.9 m s^{-1})

***(a)* Surface temperature and calculated saturation water vapor concentration as a function of freezing time**

***(b)* Integral of the saturation water vapor concentration and weight loss versus freezing time**

***(c)* Relative weight loss as a function of the integral of the saturation water vapor concentration over freezing time**

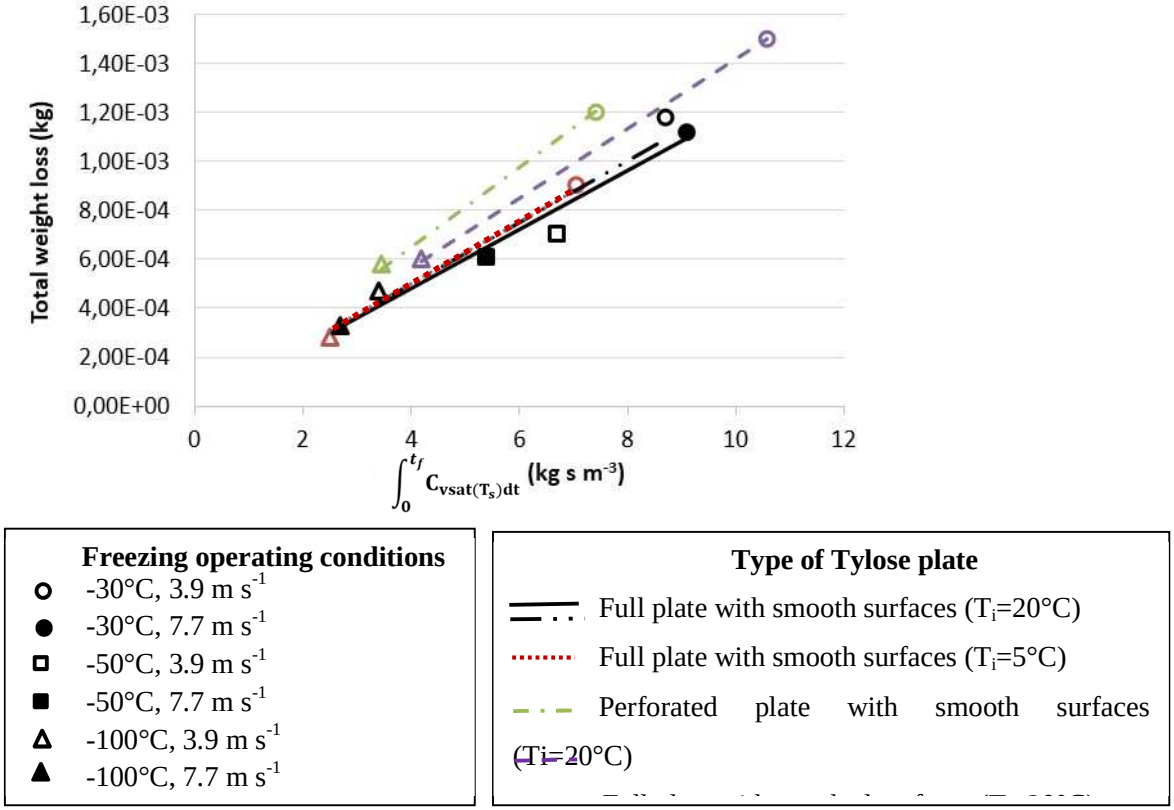

Figure 9: Total weight loss as a function of the integral of the saturation vapor concentration C_{vsat} at the product surface over the total freezing time

Table 1: Freezing operating conditions

Temperature set point (°C)	Velocity set point (m s^{-1})	Full plate with smooth surfaces T_i=20°C	Full plate with smooth surfaces T_i=5°C	Full plate with streaked surfaces T_i=20°C	Perforated plate with smooth surfaces T_i=20°C
-30	3	×3			
	3.9	×3	×1	×1	×1
	7.7	×3			
-50	3.9	×3			
	7.7	×3			
-100	3.9	×3	×1	×1	×1
	7.7	×3			

For each run, two weight loss measurements and one temperature measurement (surface and core) are carried out.

Table 2: Gas flow velocity (m s^{-1}) uniformity and stability

		Horizontal position (mm)	400 (Left)	295 (Left)	272,5 (Middle)	175 (Middle)	152,5 (Right)	52,5 (Right)	Average*
Vertical position (mm)	Upper wall	50	7,9 ± 0.1	8,5 ± 0.0	7,8 ± 0.1	8,7 ± 0.1	7,4 ± 0.1	7,1 ± 0.1	7,9 ± 0.6
	Mid-height positions	150	8,7 ± 0.1	8,8 ± 0.1	8,8 ± 0.1	8,9 ± 0.0	8,8 ± 0.1	9,1 ± 0.1	8,9 ± 0.2
		225	8,4 ± 0.1	8,9 ± 0.1	9,0 ± 0.1	8,9 ± 0.1	9.0 ± 0.1	9,0 ± 0.1	8,9 ± 0.2
		300	8,4 ± 0.1	8,9 ± 0.0	8,9 ± 0.0	8,9 ± 0.0	9.0 ± 0.1	8,9 ± 0.1	8,8 ± 0.2
	Bottom wall	400	7,9 ± 0.1	7,9 ± 0.1	8,3 ± 0.1	7,8 ± 0.0	8,5 ± 0.1	7,6 ± 0.1	8 ± 0.3

**Mean value and standard deviation of the average values at the six horizontal positions.*

Table 3: Temperature (°C) uniformity and stability

Temperature set point (°C)	Left position	Middle position	Right position	Average
0	0.0 ± 0.1	0.0 ± 0.1	0.1 ± 0.0	0.0 ± 0.1
-30	-29.9 ± 0.1	-29.8 ± 0.1	-29.8 ± 0.1	-29.8 ± 0.1
-50	-49.4 ± 0.1	-49.4 ± 0.1	-49.3 ± 0.1	-49.4 ± 0.1
-100	-99.4 ± 0.6	-99.5 ± 0.6	-99.6 ± 0.6	-99. 5 ± 0.1

Table 4: Heat transfer coefficient (W m^{-2} K^{-1}) uniformity and stability

Velocity set point (m s^{-1})	Left position	Middle position	Right position	Average
4.2	63 ± 2	59 ± 2	62 ± 2	61 ± 2
6.6	92 ± 2	84 ± 2	90 ± 3	89 ± 4
8.4	115 ± 3	101 ± 4	110 ± 4	108 ± 7

Table 5: Results of average freezing time (s) required for the thermal center of Tylose full plate with smooth surfaces (T_i=20°C) to reach -18°C

Temperature set point (°C)	Velocity set point (m s^{-1})	Left	Middle	Right	Average
-30	3	2953 ± 44	2944 ± 225	2850 ± 177	2913 ± 57 (49 min)
	3,9	2637 ± 214	2795 ± 58	2664 ± 54	2571 ± 138 (43 min)
	7,7	1728 ± 27	1727 ± 19	1700 ± 20	1718 ± 16 (29 min)
-50	3.9	1906 ± 128	1720 ± 87	1742 ± 44	1789 ± 102 (30 min)
	7.7	1179 ± 44	1301 ± 27	1191 ± 14	1224 ± 67 (21 min)
-100	3,9	807 ± 25	805 ± 30	877 ± 43	829 ± 41 (14 min)
	7,7	516 ± 55	581 ± 25	566 ± 19	554 ± 34 (10 min)

Table 6: Results of total relative weight loss according to the type of Tylose plate and freezing operating conditions (average value of replicates ± standard deviation)

Temperature set point (°C)	**Velocity set point (m s^{-1})**	**Full plate with smooth surfaces** T_I=20°C	**Full plate with smooth surfaces** **T_I=5°C**	**Full plate with streaked surfaces** **T_I=20°C**	**Perforated plate with smooth surfaces** **T_I=20°C**
-30	3	1.70 ± 0.04			
	3,9	1.61 ± 0,05	1.26 ± 0.06	1.76 ± 0.03	1.83 ± 0.02
	7,7	1.56 ± 0,07			
-50	3.9	0.98 ± 0.11			
	7.7	0.85 ± 0.15			
-100	3,9	0.71 ± 0,10	0.68 ± 0.01	0.89 ± 0.09	0.87 ± 0.02
	7,7	0.46 ± 0,03			